JOURNAL OF THE AMERICAN CHEMICAL SOCIETY

Communication

An Optical/Photoacoustic Dual Modality Probe: Ratiometric in/ex Vivo Imaging for Stimulated H2S Upregulation in Mice

Zhongyan Chen, Xueling Mu, Zhong Han, Shiping Yang,
Changli Zhang, Zijian Guo, Yang Bai, and Weijiang He

J. Am. Chem. Soc., **Just Accepted Manuscript** • DOI: 10.1021/jacs.9b09181 • Publication Date (Web): 28 Oct 2019

An Optical/Photoacoustic Dual Modality Probe: Ratiometric in/ex Vivo Imaging for Stimulated H_2S Upregulation in Mice

Zhongyan Chen,[†] Xueling Mu,[#] Zhong Han,[†] Shiping Yang,[*,#] Changli Zhang,[†] Zijian Guo,[*,†,‡] Yang Bai,[†] and Weijiang He[*,†]

† State Key Laboratory of Coordination Chemistry, Coordination Chemistry Institute, School of Chemistry and Chemical Engineering, Nanjing University, Nanjing 210023, P. R. China

‡ Chemistry and Biomedicine Innovation Center, Nanjing University， Nanjing 210023, P. R. China

Key Laboratory of Resource Chemistry, Shanghai Normal University, Shanghai, 200234, P. R. China

Supporting Information Placeholder

ABSTRACT: Tracking signaling H_2S in live mice demands responsive imaging with fine tissue imaging depth and low interferences from tissue scattering/autofluorescence and probe concentration. With complementary advantages of fluorescence and photoacoustic (PA) imaging, optical/PA dual modality imaging was suggested for in/ex vivo H_2S imaging. Therefore, a *meso*-benzoyloxyltricarboheptamethine cyanine, **HS-CyBz**, was prepared as the first ratiometric optical/PA dual modality probe for H_2S, profiting from a keto-enol transition sensing mechanism. Tail intravenous injection of this probe leads to probe accumulation in the liver of mice, and the endogenous H_2S upregulation triggered by S-adenosyl-L-methionine has been verified by ratiometric optical/PA imaging, suggesting the promising potential of this ratiometric dual modality imaging.

Many small molecule species including metal cations, reactive oxygen species, and gasotransmitters are essentially involved in signaling pathways and pathogenesis.[1,2] Beyond intracellular fluorescence imaging of signaling small molecules (SSMs),[3] in/ex vivo SSMs tracking in animal model especially in mice is appealed in pathological and clinical study. To evaluate the signaling behavior and pathology, in/ex vivo SSMs imaging is required to track SSM fluctuation besides offering SSM distribution pattern. Therefore imaging technique showing deep tissue imaging depth and SSM response is demanded. PET and SPECT are incapable to provide SSMs fluctuation information due to their irresponsive probe. Although MRI responsive probes have been reported,[4] optical imaging is more attractive for its quick response and high sensitivity.[5] However, the limited tissue penetration depth of fluorescence (<1 mm) makes optical imaging visualize only superficial SSMs. This disadvantages can be overcome by photoacoustic (PA) imaging with imaging depth of several centimeters in tissues,[6] although the sensitivity and resolution of PA imaging are lower. Therefore, fluorescence/PA dual modality imaging, which possesses the advantages of both modalities, is expected to improve SSMs imaging efficacy in mice.[7] As fluorescence and PA signals can be interfered by tissue scattering/autofluorescence and probe concentration, single channel optical and PA imaging is not reliable for tracking stimulated SSM fluctuation. Considering the advantage of ratiometric imaging in overcoming these interferences,[8] NIR ratiometric optical/PA dual modality probe is required for in/ex vivo SSM imaging.

As the third gaseous signaling molecule, H_2S is involved in vasodilation, angiogenesis, anti-oxidation, anti-inflammation, and central nervous regulation.[9] Many fluorescence probes have been developed for intracellular H_2S imaging,[10] in vivo optical or PA imaging for H_2S is still not satisfying since most of them are based on turn-on probes.[11] In this study, the first optical/PA dual modality probe showing ratiometric response to H_2S, **HS-CyBz**, was developed (Scheme 1), and in/ex vivo ratiometric optical and PA imaging for endogenous H_2S upregulation stimulated by the cystathionase activator S-adenosyl-L-methionine (SAM) was realized in mice with this probe.

Scheme 1. H_2S sensing mechanism of HS-CyBz and chemical structure of HS-CyBz-1.

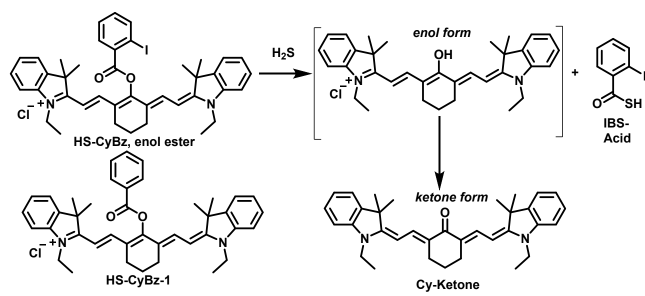

As benzoic esters of a *meso*-hydroxyltricarboheptamethine cyanine, both probe **HS-CyBz** and its analogue without ortho-iodo substituent, **HS-CyBz-1** were prepared in this study. Their cyanine moiety was adopted to provide NIR absorption and emission.[12] It is expected that nucleophilic substitution of the ester by HS^- would release enolic heptamethine cyanine, which undergoes keto-enol tautormerization to form **Cy-ketone** (Scheme 1). This tautomerization would shift emission and absorption distinctly, showing ratiometric fluorescent and photoacoustic response to HS^-. Both compounds were prepared via reacting the corresponding benzoic chloride with *meso*-hydroxyltricarboheptamethine cyanine.

Emission spectrum of **HS-CyBz** exhibits a main emission band centered at 805 nm and a minor broad band centered at 630 nm (λ_{ex}, 595 nm). Na_2S addition resulted in the drop of former band and drastic enhancement of the latter one (Figure 1a). The large hypsochromic emission shift of ~175 nm and well separated dual emission bands indicated the excellent ratiometric response behavior of **HS-CyBz** toward H_2S. A linear enhancement of emission ratio (F_{630}/F_{805}) was observed upon Na_2S titration from 0 to 1 mM (Figure S7), and the H_2S detection limit of this probe was determined to be 0.5 μM. This showed the potential of **HS-CyBz** for endogenous H_2S detection (10-600 μM in human brain, 10-100 μM in human blood[10a,13]). **HS-CyBz-1** possesses a similar emission spectrum. Temporal tracking of ratio F_{630}/F_{805} after Na_2S addition revealed that **HS-CyBz** reacted with HS^- rapidly and attained equilibrium in 10 min, while **HS-CyBz-1** reacted with HS^- much more slowly and reaction equilibrium could not be attained even after 0.5 h. Moreover, the HS^--induced ratio enhancement factor of **HS-CyBz** is much higher than that of **HS-CyBz-1** (Figure S8c). Therefore **HS-CyBz** is more suitable for H_2S sensing due to its high sensitivity and rapid response, and the electron withdrawing iodo group favoring ester cleavage via HS^- nucleophilic attacking might be the origin.

Absorption spectrum of **HS-CyBz** shows a sharp absorption band at 775 nm (ε ~ 1.8×10^5 $M^{-1}cm^{-1}$) and a shoulder band (708 nm). Probe reaction with Na_2S at pH 7.4 led to the distinct decrease of the sharp band and a minor increase at 850 nm, resulting in an isobestic point at 825 nm (Figures 1b, S8b and S9). This colorimetric sensing behavior suggested that this probe might be a ratiometric PA probe for HS^-.

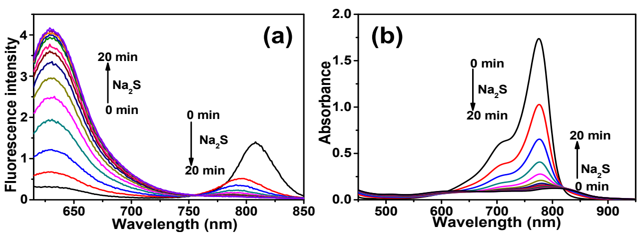

Figure 1. Emission (a, λ_{ex} 595 nm) and absorption (b) spectra of **HS-CyBz** (10 μM) in HEPES buffer (pH 7.4) determined after the addition of Na_2S (1 mM).

ESI mass determination of **HS-CyBz** solution mixed with Na_2S displayed a signal of m/z 493.25 in positive mode spectrum and a signal of m/z 262.80 in negative mode spectrum. The two signals were assigned as [**Cy-ketone**+H]$^+$ and [**IBS-Acid**-H]$^-$, respectively (Figure S10). **Cy-Ketone** has been separated from the reaction mixture in a medium yield. All these indicated that HS^- nucleophilic substitution of benzoic ester would release enolic *meso*-hydroxyltricarboheptamethine cyanine and trigger keto-enol transition, which is responsible for the HS^--induced spectroscopic response. The quantum yield of **HS-CyBz** and **Cy-Ketone** were determined as 0.02 and 0.17. The emission ratio F_{630}/F_{805} for **HS-CyBz** increased from 0.3 to 54.9 (183-fold) after 100 equiv Na_2S being added.

Investigating sensing behavior of **HS-CyBz** for biochemical species of interest revealed that only Na_2S led to a distinct enhancement of emission ratio F_{630}/F_{805} (~32-fold, 30 equiv HS^-), while other species such as cations (K^+, Na^+, Ca^{2+}, Mg^{2+}, 1 mM), anions (S_n^{2-}, 300 μM; Ac^-, HCO_3^-, NO_3^-, NO_2^-, SO_4^{2-}, SO_3^{2-}, $H_2PO_4^-$, SCN^-, $S_2O_3^{2-}$, 1 mM), reactive oxygen species (H_2O_2, ClO^-, 1 mM), biothiols (GSH, Cys, 1 mM; Hcy 200 μM), and carboxylesterase (0.5 U/mL) triggered minor change in F_{630}/F_{805}. The presence of biothiols GSH, Cys and Hcy showed no obvious interference with the HS^--induced ratio enhancement (Figure S12a). Moreover, the emission ratio F_{630}/F_{805} of **HS-CyBz** showed no distinct pH-dependence from pH 5.0 to pH 8.5 (Figure S13). The colorimetric sensing behavior suggested that this probe might enable ratiometric photoacoustic sensing for HS^-. PA imaging of **HS-CyBz** solutions revealed that the PA signal upon excitation at 825 nm (isobestic point) was weak and stable upon HS^- titration, while the signal upon excitation at 775 nm decreased distinctly in the process (Figure 2c), and the ratio PA_{825}/PA_{775} increased almost linearly from ~0.2 to ~0.7 with $[HS^-]_{total}$ increasing from 0 to 1 mM (Figure S12c). Moreover, other tested biochemical species did not induce obvious change of PA_{825}/PA_{775}, and the presence of biothiols such as GSH, Hcy and Cys did not interfere with the HS^--induced PA_{825}/PA_{775} ratio enhancement (Figures 2b and S12b), showing the ratiometric photoacoustic sensing ability for H_2S.

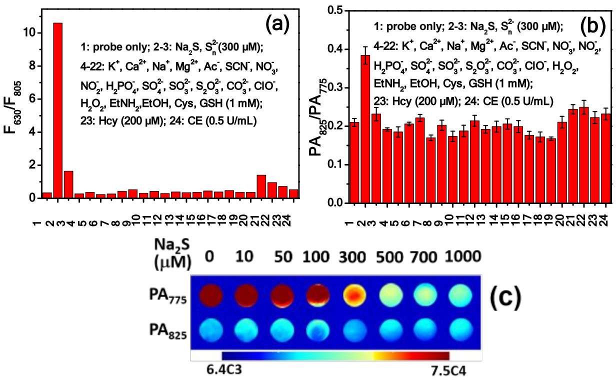

Figure 2. Emission ratio F_{630}/F_{805} (a) and PA ratio PA_{825}/PA_{775} (b) of **HS-CyBz** (10 μM) in HEPES buffer in the presence of different analytes. (c) PA image of probe (10 μM) solutions upon Na_2S titration (dual channel mode: λ_{ex} 775 and 825 nm).

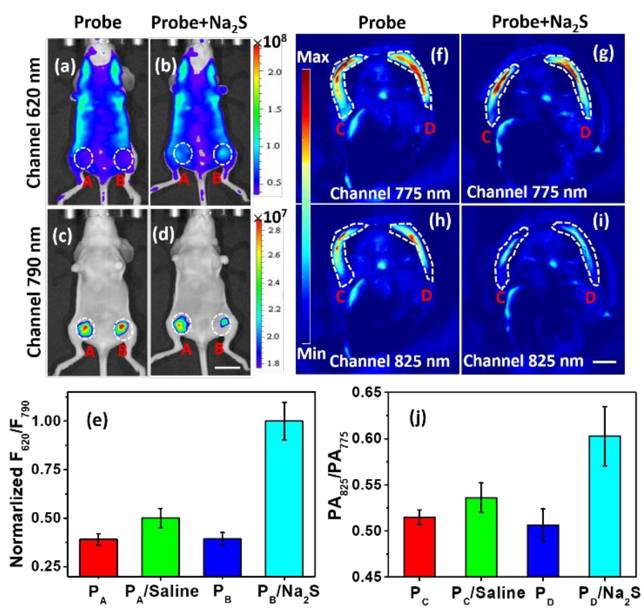

Figure 3. *In vivo* ratiometric optical (a-e, Ch 1: 620±20 nm, Ch 2: 790±20 nm, λ_{ex}, 560 nm) and PA (f-j, Ch 3: 775 nm, Ch 4: 825 nm) imaging for H_2S in mice injected subcutaneously with **HS-CyBz** (P, 100 μL, 20 μM) in region of interests (A, B on the hind limbs; C, D on the back). (a, c) Images of probe-injected mouse; (b, d) images of mouse in (a, c) 30 min post saline (ROI A) and Na_2S (ROI B) injection (100 μL, 1 mM); (e) normalized F_{620}/F_{790} of ROIs A and B determined in (a-d). Scale bar: 1 cm. (f, h) PA images of probe-injected mouse; (g, i) PA images of mouse in (f, h) 30 mins post injection with saline (ROI C) and Na_2S (ROI D); (j) PA_{825}/PA_{775} ratios for ROIs C and D. Scale bar: 3 mm.

Without commercial available apparatus uniting optical and PA imaging, ratiometric optical and PA imaging ability of **HS-CyBz** for H_2S were investigated in mice, respectively. In vivo ratiometric optical imaging was realized initially in a 6-week-old mouse with the hind limbs being injected with probe subcutaneously (ROIs A and B). The image from channel 1 (620±20 nm) showed that the weak fluorescence of free probe in ROIs A and B was almost concealed by tissue autofluorescence. The subsequent Na_2S injection in ROI B led to the fluorescence enhancement (~1.60-fold, Figures 3b and S14a), which was still interfered by tissue autofluorescence. The control (ROI A) injected with saline showed a less enhancement factor of ~1.21-fold. Images from Channel 2 (790±20 nm) showed no obvious autofluorescence interference, and Na_2S injection led to fluorescence decrease with a factor of ~0.63-fold, and that for control (ROI A) was ~0.94-fold. Therefore, Na_2S injection in ROI B made fluorescence ratio F_{620}/F_{790} increase with a factor of ~2.54-fold, indicating the enhanced HS^- concentration. The control in ROI A showed a minor ratio enhancement factor of ~1.28-fold (Figure 3e). The Na_2S-induced F_{620}/F_{790} change in ROI B is more distinct than the single channel signal change (F_{620}). This result indicated that in vivo ratiometric optical imaging is more reliable and sensitive than single channel turn-on imaging, and the interference from autofluorescence and deviated probe concentration is effectively reduced.

The dual channel photoacoustic imaging was carried out on the back of mouse with ROIs C and D injected subcutaneously with the probe. The distinct photoacoustic signals of the probe were observed in both channels (Figures 3f and 3h, ROIs C and D) with Channel 4 showing the lower signal. The signal ratio PA_{825}/PA_{775} for both ROIs C and D with only probe injection is similar (~0.51, Figures S14b and 3j). The subsequent Na_2S injection in ROI D made the signal in both channels decrease (Figures 3g and 3i), which is different from the expected signal decrease in Channel 3 and stable signal in Channel 4. The local probe concentration decrease caused by diffusion and the injection-induced dilution may be the origin. However, ratio PA_{825}/PA_{775} of ROI D was enhanced to 0.60 upon Na_2S injection (Figure 3j), while that for control in ROI C with saline injection was 0.53. This confirmed that the HS^- level in ROI D was enhanced. All results revealed that the ratiometric PA imaging is more reliable than single channel PA imaging in reducing interference from the deviated local probe concentration.

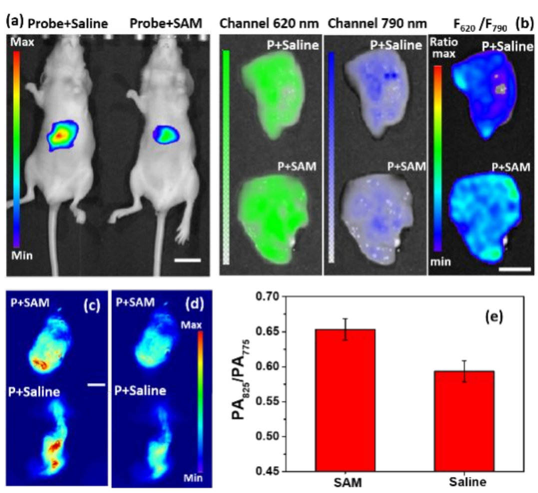

Figure 4. Optical (a-b) and photoacoustic (c-e) imaging for mice injected with SAM. **HS-CyBz** was injected intravenously 12 h post SAM injection. (a) Fluorescence image of mice injected with SAM and saline. Bandpath 790±20 nm, λ_{ex} 720 nm; (b) ex vivo fluorescence images of isolated livers from mouse in (a) acquired at 620 (left) and 790 (middle) nm, and ratiometric image (right), λ_{ex} 560 nm; Scale bar, 1 cm. (c-d) PA images of livers from the SAM- and saline-injected mice recorded by channel 775 nm (c) and channel 825 nm (d), and the related PA_{775}/PA_{825} ratios (e). Scale bar, 6 mm.

In/ex vivo imaging for endogenous H_2S upregulation in mice was explored, and SAM was utilized to upregulate H_2S expression.[14] The mouse was injected intravenously with **HS-CyBz** 12 h post SAM intraperitoneal injection. Optical imaging revealed that the fluorescence in the epigastrium of SAM-injected mouse was much lower than that in mouse with saline injection, implying SAM-injection enhanced H_2S level distinctly (Figure 4a). The ex vivo optical imaging of isolated viscera disclosed the liver accumulation of this probe (Figure S15), and ex vivo ratiometric image revealed that F_{620}/F_{790} ratio in the liver of SAM-injected mouse was distinctly higher than that in mouse with no SAM injection (Figure 4b), confirming SAM-injection inducing endogenous H_2S enhancement in the liver. As shown in single channel PA images of the isolated livers (Figures 4c and 4d), it is difficult to judge whether SAM-injection trigger H_2S upregulation in liver. However, the PA signal ratio PA_{825}/PA_{775} was enhanced from 0.59 in the liver of saline-injected mouse to 0.65 in the liver of SAM-injected mouse (Figure 4e). This result indicated that SAM injection caused H_2S upregulation, confirming the advantage of dual channel ratiometric PA imaging.

In summary, the first ratiometric optical/PA dual modality probe for H_2S was prepared, profiting from the HS^--induced keto-enol tautormerization of *meso*-hydroxyltricarboheptamethine cyanine. With NIR absorption/emission, **HS-CyBz** enables the optical/photoacoustic dual modality imaging for subcutaneous H_2S in mice, and the ratiometric imaging for both modes favors the alleviation of interferences from tissue autofluorescence and the deviated probe concentration. Tail intravenous injection of probe resulted in accumulation in mice liver, and the SAM-stimulated endogenous H_2S enhancement in the liver was confirmed by optical/PA dual modality imaging. This study indicates that ratiometric optical/PA dual modality imaging was an effective approach to tracking SSM upregulation in live mice and tissues, and the perspective technique uniting optical and PA imaging should promote SSM biology in the future.

ASSOCIATED CONTENT

Supporting Information

The Supporting Information is available free of charge on the ACS Publications website. Synthesis, characterization of probe and experiment details for spectroscopic and imaging study.

AUTHOR INFORMATION

Corresponding Author

*shipingy@shnu.edu.cn
*zguo@nju.edu.cn
*heweij69@nju.edu.cn

Notes

The authors declare no competing financial interests.

ACKNOWLEDGMENT

We thank the National Basic Research Program of China (No. 2015CB856300) and National Natural Science Foundation of China (No. 21571099, 21977044 and 21731004) for financial support.

REFERENCES

(1) (a) Chang, C. J. Searching for harmony in transition-metal signaling. *Nat. Chem. Biol.* **2015**, *11*, 744-747; (b) Pablos, P.; Mendiguren, A.; Pineda, J. Contribution of nitric oxide-dependent guanylate cyclase and reactive oxygen species signaling pathways to desensitization of mu-opioid receptors in the rat locus coeruleus. *Neuropharmacology* **2015**, *99*, 422-431; (c) Wang, R. Shared signaling pathways among gasotransmitters. *Proc. Natl. Acad. Sci. USA* **2012**, *109*, 8801-8802; (d) Klein, M. O.; Battagello, D. S.; Cardoso, A. R.; Hauser, D. N.; Bittencourt, J. C.; Correa, R. G. Dopamine: functions, signaling, and association with neurological diseases. *Cell. Mol. Neurobiol.* **2019**, *39*, 31-59.

(2) (a) Leal, S. S.; Botelho, H. M.; Gomes, C. M. Metal ions as modulators of protein conformation and misfolding in neurodegeneration. *Coord. Chem. Rev.* **2012**, *256*, 2253-2270; (b) Harrison, I. P.; Selemidis, S. Understanding the biology of reactive oxygen species and their link to cancer: NADPH oxidases as novel pharmacological targets. *Clin. Exp. Pharmacol. Physiol.* **2014**, *41*, 533-542; (c) Szabo, C. Gasotransmitters in cancer: from pathophysiology to experimental therapy. *Nat. Rev. Drug Discov.* **2016**, *15*, 185-203.

(3) (a) Chen, Y.; Bai, Y.; Han, Z.; He, W.; Guo, Z. Photoluminescence imaging of Zn^{2+} in living systems. *Chem. Soc. Rev.* **2015**, *44*, 4517-4546; (b) Lee, M. H.; Kim, J. S.; Sessler, J. L. Small molecule-based ratiometric fluorescence probes for cations, anions, and biomolecules. *Chem. Soc. Rev.* **2015**, *44*, 4185-4191.

(4) (a) Al-Karmi, S.; Albu, S. A.; Vito, A.; Janzen, N.; Czorny, S.; Banevicius, L.; Nanao, M.; Zubieta, J.; Capretta, A.; Valliant, J. F. Preparation of an (18) F-labeled hydrocyanine dye as a multimodal probe for reactive oxygen species. *Chem. Eur. J.* **2017**, *23*, 254-258; (b) Que, E. L.; Chang, C. J. Responsive magnetic resonance imaging contrast agents as chemical sensors for metals in biology and medicine. *Chem. Soc. Rev.* **2010**, *39*, 51-60; (c) Zhang, X.; Lovejoy, K. S.; Jasanoff, A.; Lippard, S. J. Water-soluble porphyrins as a dual-function molecular imaging platform for MRI and fluorescence zinc sensing. *Proc. Natl. Acad. Sci. USA*. **2007**, 104, 10780-10785.

(5) (a) Weissleder, R. A clearer vision for in vivo imaging. *Nat. Biotechnol.* **2001**, *19*, 316-317; (b) Hammers, M. D.; Taormina, M. J.; Cerda, M. M.; Montoya, L. A.; Seidenkranz, D. T.; Parthasarathy, R.; Pluth, M. D. A Bright fluorescent probe for H_2S enables analyte-responsive, 3D imaging in live zebrafish using light sheet fluorescence microscopy. *J. Am. Chem. Soc.* **2015**, *137*, 10216-10223; (c) Chen, F.; Xiao, F.; Zhang, W.; Lin, C.; Wu, Y. Highly stable and NIR luminescent Ru-LPMSN hybrid materials for sensitive detection of Cu^{2+} in vivo. *ACS Appl. Mater. Interfaces* **2018**, *10*, 26964-26971.

(6) (a) Wang, L. V.; Hu, S. Photoacoustic tomography: in vivo imaging from organelles to organs. *Science* **2012**, *335*, 1458-1462; (b) Nie, L.; Chen, X. Structural and functional photoacoustic molecular tomography aided by emerging contrast agents. *Chem. Soc. Rev.* **2014**, *43*, 7132-7170; (c) Chen, Q.; Liang, C.; Sun, X.; Chen, J.; Yang, Z.; Zhao, H.; Feng, L.; Liu, Z. H_2O_2-responsive liposomal nanoprobe for photoacoustic inflammation imaging and tumor theranostics via in vivo chromogenic assay. *Proc. Natl. Acad. Sci. USA* **2017**, *114*, 5343-5348; (d) Li, X.; Kim, J.; Yoon, J.; Chen, X. Cancer-associated, stimuli-driven, turn on theranostics for multimodality imaging and therapy. *Adv. Mater.* **2017**, 1606857.

(7) Anees, P.; Joseph, J.; Sreejith, S.; Menon, N. V.; Kang, Y.; Wing-Kwong Yu, S.; Ajayaghosh, A.; Zhao, Y. Real time monitoring of aminothiol level in blood using a near-infrared dye assisted deep tissue fluorescence and photoacoustic bimodal imaging. *Chem. Sci.* **2016**, *7*, 4110-4116.

(8) (a) Huang, X.; Song, J.; Yung, B. C.; Huang, X.; Xiong, Y.; Chen, X. Ratiometric optical nanoprobes enable accurate molecular detection and imaging. *Chem. Soc. Rev.* **2018**, *47*, 2873-2920; (b) Zhou, J.; Ma, H. Design principles of spectroscopic probes for biological applications. *Chem. Sci.* **2016**, *7*, 6309-6315.

(9) (a) Yang, G., Wu, L.; Jiang, B.; Yang, W.; Qi, J., Cao, K.; Meng, Q.; Mustafa, A. K.; Mu, W.; Zhang S. Snyder, S. H.; Wang, R. H_2S as a physiologic vasorelaxant: hypertension in mice with deletion of cystathionine γ-lyase. *Science* **2008**, 322, 587-590; (b) Szabo, C. Hydrogen sulphide and its therapeutic potential. *Nat. Rev. Drug Discov.* **2007**, *6*, 917-935.

(10) (a) Chen, Y.; Zhu, C.; Yang, Z.; Chen, J.; He, Y.; Jiao, Y.; He, W.; Qiu, L.; Cen, J.; Guo, Z. A ratiometric fluorescent probe for rapid detection of hydrogen sulfide in mitochondria. *Angew. Chem. Int. Ed.* **2013**, *52*, 1688-1691; (b) Lin, V. S.; Chen, W.; Xian, M.; Chang, C. J. Chemical probes for molecular imaging and detection of hydrogen sulfide and reactive sulfur species in biological systems. *Chem. Soc. Rev.* **2015**, *44*, 4596-4618; (c) Chen, M.; Chen, R.; Shi, Y.; Wang, J.; Cheng, Y., Li, Y.; Gao, X.; Yan, Y.; Sun, J. Z.; Qin, A.; Kwok, R. T. K.; Lam, J. W. Y.; Tang, B. Z. Malonitrile-Functionalized Tetraphenylpyrazine: Aggregation-Induced Emission, Ratiometric Detection of Hydrogen Sulfide, and Mechanochromism *Adv. Funct. Mater.* **2018**, 1704689; (d) Zhao, C.; Zhang, X.; Li, K.; Zhu, S.; Guo, Z.; Zhang, L.; Wang, F.; Fei, Q.; Luo, S.; Shi, P.; Tian, H.; Zhu, W.-H. Förster Resonance Energy Transfer Switchable Self-Assembled Micellar Nanoprobe: Ratiometric Fluorescent Trapping of Endogenous H_2S Generation via Fluvastatin-Stimulated Upregulation. *J. Am. Chem. Soc.* **2015**, *137*, 8490-8498; (e) Zhao, B.; Yang, B.; Hu, X.; Liu, B. Two colorimetric and ratiometric fluorescence probes for hydrogen sulfide based on AIE strategy of α-cyanostilbenes. *Spectrochim. Acta A* **2018**, *199*, 117-122.

(11) (a) Zhang, K.; Zhang, J.; Xi, Z.; Li, L. Y.; Gu, X.; Zhang, Q. Z.; Yi, L. A new H_2S-specific near-infrared fluorescence-enhanced probe that can visualize the H_2S level in colorectal cancer cells in mice. *Chem. Sci.* **2017**, *8*, 2776-2781; (b) Chen, W.; Xu, S.; Day, J. J.; Wang, D.; Xian, M. A General Strategy for Development of Near-Infrared Fluorescent Probes for Bioimaging. *Angew. Chem. Int. Ed.* **2017**, *56*, 16611-16615.

(12). Sun, W.; Guo, S.; Hu, C.; Fan, J.; Peng, X. Recent development of chemosensors based on cyanine platforms. *Chem. Rev.* **2016**, *116*, 7768-7817.

(13) Peng, H.; Cheng, Y.; Dai, C.; King, A. L.; Predmore, B. L.; Lefer, D. J.; Wang, B. A Fluorescent Probe for Fast and Quantitative Detection of Hydrogen Sulfide in Blood. *Angew. Chem. Int. Ed.* **2011**, *50*, 9672-9675.

(14) Prudova, A.; Bauman, Z.; Braun, A.; Vitvitsky, V.; Lu, S. C.; Banerjee, R. S-adenosylmethionine stabilizes cystathionine β-synthase and modulates redox capacity. *Proc. Natl. Acad. Sci. USA* **2006**, *103*, 6489-6494.

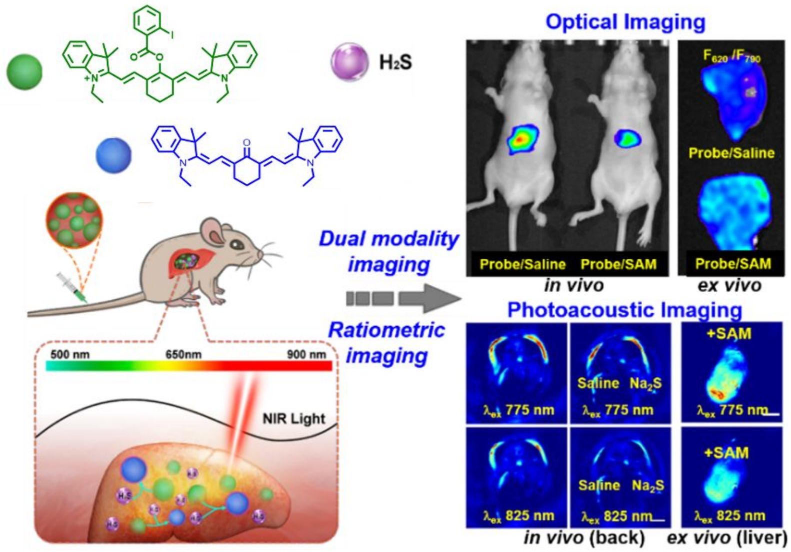

H2S
Optical Imaging
F620/F790
Probe/Saline
Probe/Saline
Probe/SAM
Probe/SAM
in vivo
ex vivo
Dual modality imaging
Ratiometric imaging
500 nm
650nm
900 nm
NIR Light
Photoacoustic Imaging
+SAM
Saline
Na2S
λex 775 nm
λex 825 nm
in vivo (back)
ex vivo (liver)